Journal of Water Resources and Ocean Science
2024, Vol. 13, No. 4, pp. 105-115
https://doi.org/10.11648/j.wros.20241304.12

Research Article

Hydrogeological Characterisation of a Sedimentary Aquifer and Springs Near the City of Bobo-Dioulasso, Burkina Faso: Isotopic Approaches

César Millogo[1, 2, *], Issan Ki[2], Issoufou Ouedraogo[2, 3], Samuel Nakolendousséé[2]

[1]Applied Science and Technology Training and Research Unit, Daniel OUEZZIN-COULIBALY University, Dédougou, Burkina Faso

[2]Geosciences and Environment Laboratory, Department of Earth Sciences, Joseph Ki-Zerbo University, Ouagadougou, Burkina Faso

[3]Mining Engineering Department, Yembila-Abdoulaye-TOGUYENI University, Fada N'Gourma, Burkina Faso

Abstract

The aim of this study was to gain a better understanding of the functioning of the aquifer system and springs in the Pala basin through hydrochemical and isotopic analyses. Thirteen samples were analyzed, including two rainwater samples, three spring samples and eight borehole samples. The stable isotopic composition (^{2}H and ^{18}O) of rainwater shows that it is virtually unaffected by evaporation as it falls. Groundwater d-excess values are high, with an average of 11.28 ‰, and all samples have values higher than the local rainfall average of 7.99 ‰. This result suggests direct infiltration of precipitation of oceanic and slightly continental origin, through a favourable geological context. The isotopic study shows that there are two different recharge periods: a cold, wet period with a depletion in ^{18}O and the current period. Around borehole E2, the oldest with a tritium content of 1.8 TU, recharge took place during this cold period. The other waters are the result of mixing with waters from the current period. The springs observed in the study area come from Sotouba sandstone aquifers after erosion exposed the piezometric water level in the Kou basin, hence their origin. Most of the boreholes tap the aquifers of both geological formations, which makes it difficult to distinguish the water from these two aquifers by analysis.

Keywords

Pala, Taoudéni, Isotopic, Spring, Groundwater, Recharge

1. Introduction

To investigate hydrogeological processes such as recharge rates, flow exchange, origins of springs, and groundwater residence times, isotopic techniques are used despite the variability of hydrogeological contexts [1-7].

Commonly used radioactive isotopes (^{3}H and ^{14}C) and stable isotopes ($\delta^{2}H$, $\delta^{18}O$) are effective in identifying groundwater origins [8-11].

Many studies around the world have used radioactive iso-

*Corresponding author: cesardmillogo@yahoo.com (César Millogo)

Received: 11 September 2024; **Accepted:** 6 October 2024; **Published:** 31 October 2024

topes (^{3}H and ^{14}C) to estimate old and new recharge and estimate the groundwater renewal time [12-15]. Sometimes, isotopic techniques and hydrogeochemical data are combined to estimate recharge sources and residence times to determine water vulnerability to pollution [3, 16-19].

This is the case of [3] who combined stable (^{18}O and ^{2}H) and radioactive isotopes (^{3}H and ^{14}C) and hydrochemical (EC, HCO_3^-, Cl^-, NO_3^-) to show the characteristics (recharge, residence time, etc.) of the Douala aquifer in Cameroon.

In the locality of Pala located less than a kilometre south-east of Bobo Dioulasso, there are three (03) springs close to the catchment boreholes of ONEA. These springs are permanent and flow all year round without interruption.

This raises the question of the true origin of these water sources. Do they come from fossil aquifers or recent infiltrations? What is the link between these sources and the ONEA boreholes?

There are practically no studies on these sources and the aquifers captured by ONEA drilling. The studies that exist in the area are global and mainly focus on the southeastern edge of the Taoudéni basin in Burkina Faso [2, 20-24]. The knowledge about groundwater flow conditions within the STBA is relatively limited with very little information on potentiometric heads, recharge processes, residence time and water quality [25]. Not only are there very few boreholes in the area, but they are also less than 200 meters deep, making it difficult to understand the overall structure of the aquifers [22]. Given the importance of these aquifers in supplying the city of Bobo Dioulasso with drinking water, it is essential to continue research to gain a better understanding of their functioning for sustainable management. To achieve this, water samples were taken from the springs and all existing boreholes for hydrochemical and isotopic analysis, with the aim of understanding how the aquifers in the area function.

2. Geographical and Geological Context

2.1. Geography of Study Area

The study area is located in Pala, south-east of Bobo Dioulasso, the economic capital of Burkina Faso (Figure 1). This is a Sudanian climate zone, with two contrasting seasons: a rainy season from May to October and a dry season from November to April. Average monthly temperatures range from 25 ℃ to 31 ℃. The region is characterized by two high-temperature peaks (March and October) and two low temperature peaks (July and December). Annual potential evapotranspiration in the area varied between 1,800 and 2,150 mm/year according to ANAM, depending on the method used and the measurement site (Figure 2).

It has an altitude of around 400 m on the edge of the Taoudéni sedimentary basin. To the south-west of the area, the topography rises to an altitude of around 500 meters and is fairly rugged. By contrast, the altitude drops to 300 meters in the south-east in the crystalline terrain. Moving north-eastwards, erosion is increasingly evident in a general reduction in altitude to 280 m at the mouth of the Mouhoun, a widening of the valleys and a reduction in the slopes of the hillsides. Three springs are visible in the study area and feed the hydrographic network of the Bougouriba catchment (Figure 3).

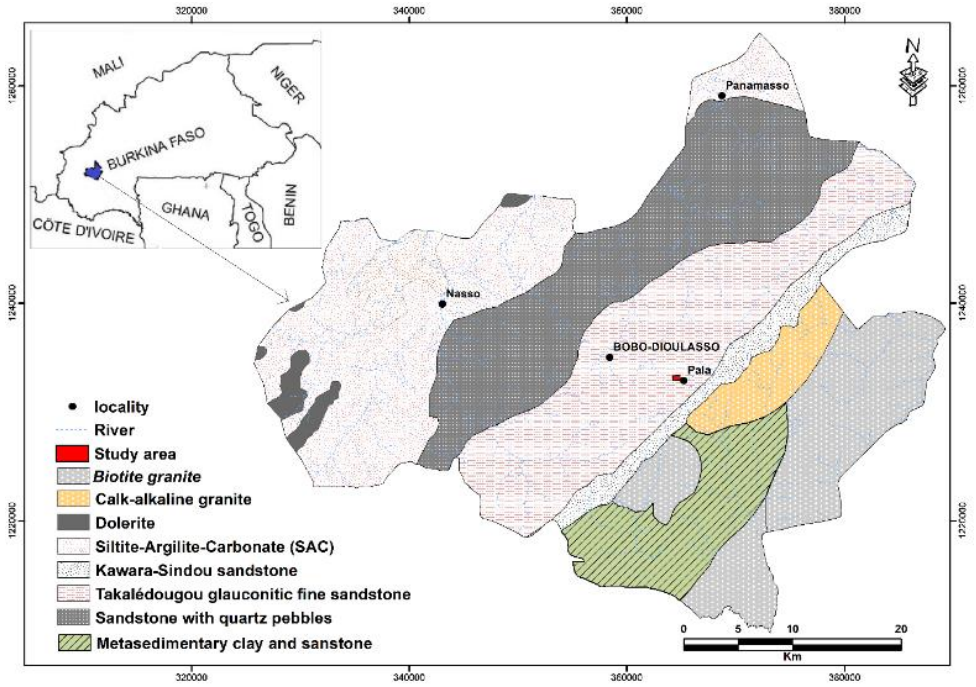

Figure 1. *Location and geological map.*

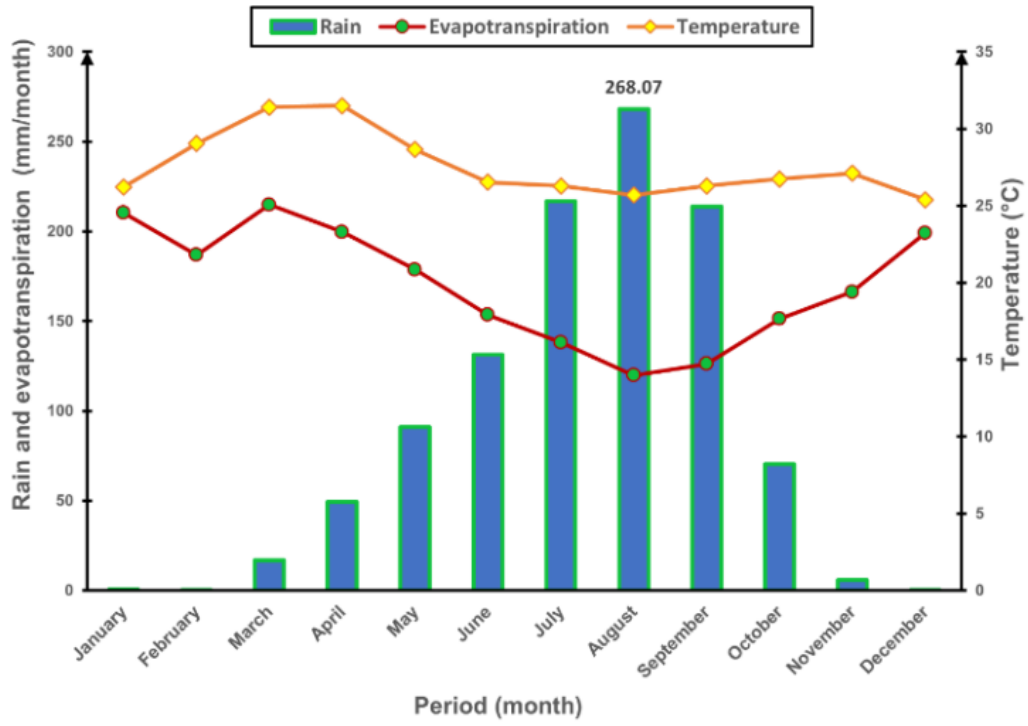

Figure 2. *Average monthly rainfall, temperature and evapotranspiration at Bobo Dioulasso meteorological station from 2000 to 2022 (Source: ANAM, 2022).*

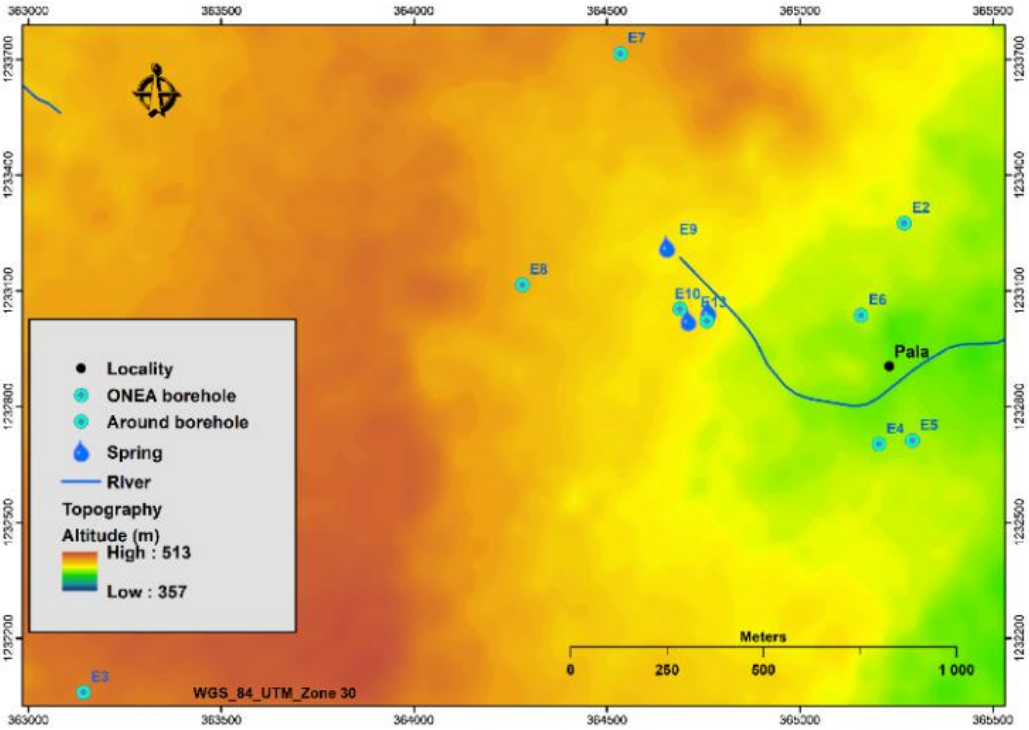

Figure 3. *Study areas showing boreholes and springs location and altitude (m).*

2.2. Geological Context

The only dating available for the sedimentary series of the Taoudéni Basin in Burkina Faso comes from a palaeomagnetic study that estimates the sandstones of the Takalédougou Formation at 775 ± 52 Ma [21]. The study area is unconformably overlain by the Neoproterozoic to Phanerozoic sediments of the Taoudéni basin [26]. Its geological formations (Figure 1) are part of the lower group according to the stratigraphic division

established by [23]. They include:

1) The Lower Sandstone Formation, located exclusively in the Banfora tongue. This is the first formation in the lower group of the sedimentary series. The known extent of these sandstones theoretically does not extend beyond the Banfora region; however, certain arguments (coloration and presence of fractured zones) suggest that there could be fragments near Pala, at the foot of the cliff, or in the Kangoura and Bagué ra "tongues."
2) The Kawara-Sindou sandstone, which comprises two facies that are more or less easy to distinguish: at the base, the coarse Sindou facies, which reduces considerably in thickness from west to east, and at the top, the Sindou facies, which is more constant in thickness and has a characteristic ruiniform appearance on outcrop. Although it does not outcrop directly in the area of the ONEA boreholes, it is found further to the south-east, resting on the crystalline basement.
3) The lower part of the Takalédougou glauconitic fine sandstone, also known as the Sotouba sandstone consists of alternating coarse glauconitic conglomeratic sandstones and thin layers of very fine, silty sandstones with a shaly flow [22, 27]. It outcrops in a thin band on the edge of the cliff (Toussiana) or set back (Darsalamy). Sometimes, as at Pala, the fine glauconitic sandstones form a redan a few tens of meters high upstream of the cliff itself, which is formed by the underlying sandstones. There are NESW and NWSE fractures. This has been confirmed by structural measurements on outcrops (Figure 4).

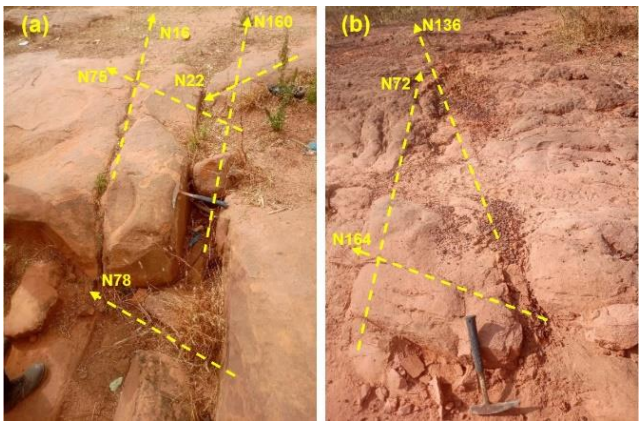

Figure 4. *Structural directions measured in situ. (a) on sotouba sandstone; (c)on laterite.*

The presence of a network of faults in different directions encourages the circulation of water at depth and could create significant interconnections between the different aquifers. In the catchment, the alterites are waterlogged at the surface, but there is an unsaturated zone between these waterlogged alterites and the deep aquifers. The Sotouba sandstone aquifers are exploited by boreholes in districts such as Flakin and Sector 25 of Bobo. These boreholes are no more than 115 m deep. Beneath the Sotouba sandstone aquifers lie the Kawara Sindou sandstone aquifers, which are not visible on the surface of the basin in the study area. These Kawara Sindou sandstone aquifers are exploited by deep boreholes drilled by ONEA, the Konsilalo school in Pala and a few private boreholes. To exploit the aquifers of Kawara Sindou sandstone, boreholes at least 120 m deep are required. The piezometric gradient is highly variable (5.10^{-4} to 10^{-1}). However, it is of the order of 10^{-2} at the Kawara Sindou sandstone level tapped by ONEA boreholes. The few measurements of piezometric level altitudes show variations ranging from 381 to 384 m. This results in a low piezometric gradient and therefore a low water flow velocity.

3. Sampling Strategy and Analytic Methods

3.1. Sampling Strategy

3.1.1. Precipitation Sample and Data one Climate Characteristics

From June to October 2022, rainwater was collected, resulting in two samples (Table 1). The first sample covers the beginning of the rainy season (June to August), while the second sample represents the end of the season (September to October).

Table 1. *Variation in dissolved oxygen isotope values in Pala precipitation.*

Variables	Min	Max	Mean	SD
Precipitation during June to September 2022 (N=2)				
δ^2H (V-SMOW)	-62.4	-16.5	-39.45	32.46
$\delta^{18}O$ (V-SMOW)	-8.85	-3.01	-5.93	4.13
Dissolved oxygen	7.25	7.50	7.38	0.18
^3H	5.00	5.50	5.23	0.33

3.1.2. Groundwater Sampling

Sampling for isotopic analyses (δ^2H, $\delta^{18}O$ and ^3H) were collected during field campaigns in October 2022 (end of the rainy season). During this campaign, water samples were collected from existing boreholes and springs. All samples were collected in 1000 mL hermetically sealed polyethylene bottles for 1000 mL for the δ^2H, $\delta^{18}O$, and ^3H analysis. A total of 9 samples (Table 2) were collected for isotopic analyses: 3 from springs and 6 from boreholes.

Table 2. *Variation in dissolved oxygen isotope values in Pala groundwater.*

Variables	Min	Max	Mean	SD
Borehole N=6				
δ^2H (V-SMOW)	-39.00	-26.00	-29.11	4.22
$\delta^{18}O$ (V-SMOW)	-5.95	-4.68	-5.07	0.41
Dissolved oxygen	5.48	6.82	6.34	0.45
^3H	0.10	2.50	1.83	0.98
Spring N=3				
δ^2H (V-SMOW)	-27.7	-27.4	-27.57	0.15
$\delta^{18}O$ (V-SMOW)	-4.99	-4.57	-4.82	0.22
Dissolved oxygen	5.85	6.52	6.17	0.34
^3H	2.00	3.70	2.81	1.20

3.2. Analytic Sampling

To determine the δ^2H and $\delta^{18}O$ contents in the water samples, analyses were carried out using laser spectroscopy at the LRAE of the Ecole Nationale d'Ingénieurs de Sfax in Tunisia. These stable isotope contents of stable isotopes (δ^2H and $\delta^{18}O$) were determined using an LGR laser spectrometer. Measurements are expressed in δ (‰) relative to the international standard V-SMOW (Vienna Standard Mean Ocean Water), which represents the average composition of oceanic waters. The analytical errors on the measurements are ±0.1 ‰ for ^{18}O and ± 1 ‰ for ^2H. The equation from the research of T. B. Coplen was used to calculate the δ values is:

$$\delta = [\left(\frac{R_S}{R_V} - SMOW\right) - 1]\times 1{,}000 \quad (1)$$

where RS represents either the or the $^{18}O/^{16}O$ or the $^2H/^1H$ ratio of the sample, and RV-SMOW is either the $^{18}O/^{16}O$ or the $^2H/^1H$ ratio of the V-SMOW [28]. For rain, there is a linear relationship between the oxygen-18 concentration and the deuterium concentration [29, 30]. This relationship expresses the straight line of meteoric water which on a global scale is as follows:

$$\delta 2H = 8\delta 2O + 10‰ \quad (2)$$

Local analysis of the relationship between oxygen (^{18}O ‰) and deuterium (^2H in ‰) allows us to identify water that has undergone a process of evaporation and/or a process of mixing [1].

Tritium (^3H) analyses were carried out using a liquid scintillation counter following electrolytic enrichment of the water samples at the LRAE of the Ecole Nationale d'Ingénieurs de Sfax in Tunisia. The concentrations are expressed in tritium units (TU) with an accuracy of ± 0.3 TU.

Major chemical parameters were analyzed using titrimetric (HCO_3 and colorimetry methods (Cl^-, NO_3^- and SO_4^{2-}) at the hydrochemistry laboratory of DGRE in Ouagadougou/Burkina Faso. Electrical conductivity (EC) was measured with a multiparameter probe (Consort C 931type) during field sampling.

4. Results

4.1. Stable Isotopes in the Study Area

4.1.1. Precipitation

The large standard deviation (32.46‰ for δ^2H and 4.13‰ for $\delta^{18}O$) relative to their respective mean value (-39.45‰ for δ^2H and -5.93‰ for $\delta^{18}O$) indicates that the isotopic composition of rainfall events varied widely (Table 1).

The two LMWLs are almost identical and close to the GMWL (GMWL: $\delta^2H = 8\ \delta^{18}O + 10‰$) [29]. This suggests that precipitation in the tropical study area occurred under equilibrium conditions [30] primarily from the atmospheric vapor of oceanic origin.

The stable isotopic composition of rainwater from the locality indicates a variance of -8.85 to -3.01‰ VSMOW in $\delta 1^8O$ values, with a mean value of -5.93‰, and from -62.4 to -16.5‰ VSMOW for δ^2H, with an average value of -39.45‰. These results are consistent with isotope studies of rainwater in the region [31, 32] and also match those found by [5, 33] as part of the IAEA project RAF7021. Furthermore, the slope 7.8 (Figure 5) of current rains very close to that of the GMWL slope 8 (Table 3) shows that these waters are practically not affected by phenomena evaporations during their fall. Unlike the rainfall events of September-October, a depletion of ^{18}O and ^3H is observed in the rainwater of July-August. This may be explained by the heavy rains that occurred during this period. Indeed, high rainfall tends to produce water that is more depleted in heavy isotopes than low rainfall. The induced stable isotope enrichment of water due to evaporation is linked to fractionation processes affected by altitude and seasonal temperature variations [34-37].

Table 3. *Table comparing the equations of the global meteoric line and some local meteoric lines in Burkina Faso*

Line	Locality	Equation of the line	Reference
GMWL	Global scale	$\delta^2H = 8\ \delta^{18}O + 10$	Craig (1961)

Line	Locality	Equation of the line	Reference
LMWL 1	Burkina Faso (Centre West	$\delta^2H = 7,7\ \delta^{18}O + 12$	Koussoub é(2010)
LMWL 2	Burkina Faso (South West)	$\delta^2H=7,18\delta^{18}O+ 7,51$	Ki (2023)
LMWL 3	Burkina Faso (West)	$\delta^2H = 7,9\ \delta^{18}O + 7,2$	Millogo (2024)

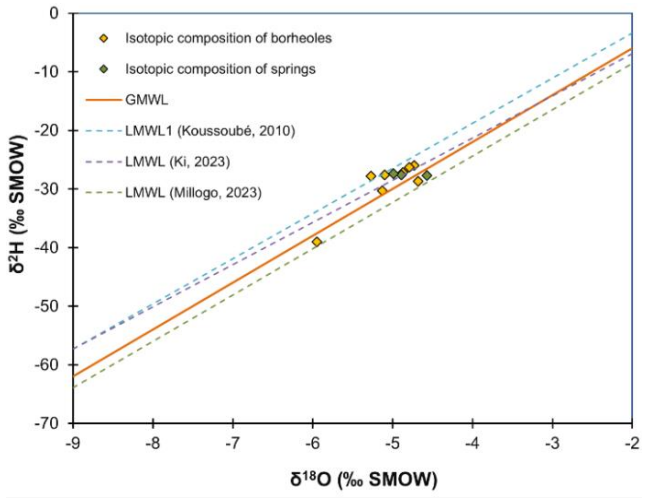

Figure 5. *Conventional diagram of δ^2H versus $\delta^{18}O$ in groundwater and spring.*

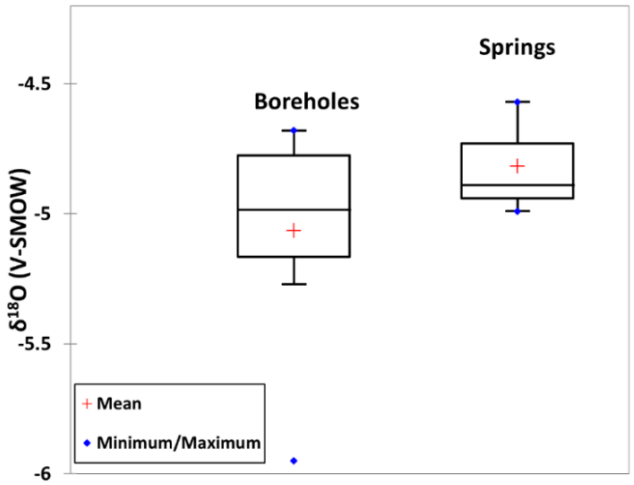

Figure 6. *Box plots show the variation in $\delta^{18}O$ among samples from the springs and boreholes.*

4.1.2. Water Sources and Groundwater

To understand the origin of water from boreholes and springs in the studied area, we draw inspiration from the δ^2H - $\delta^{18}O$ diagram, which shows the main variations observed in relation to global and local precipitation lines, the system's input signal [38, 39].

In boreholes water samples, $\delta^{18}O$ ranges from -5.95 to -4.68‰ with a mean of -5.01‰ and δ^2H ranges from, -39 to -26‰ with a mean of -29.11. On the other hand, in springs, $\delta^{18}O$ ranges from -4.99 to-4.57‰ with a mean of -4.82‰ and δ^2H ranges from, -27.7 to -27.4‰ with a mean of -27.57‰ (Table 2). It should be noted that the values are concentrated around the mean, as shown in the diagram (Figure 6).

The $^2H/^{18}O$ relationship in groundwater (boreholes and springs) shows that most of the points are organized around the local meteoric lines (LMWL1 and LMWL 2) and the global meteoric line (GMWL) (Figure 6). Their signature is therefore close to that of current rainwater in the study area. These waters result from a direct and rapid infiltration of rainwater very little influenced by evaporation phenomena. However, the water from borehole E2 shows the most depleted contents in ^{18}O and ^2H. These waters certainly come from a direct and rapid recharge of the aquifer by rainwater depleted in heavy isotopes and/or from a mixture of ancient waters [15, 36].

Principal component analysis (PCA), based on stable (^2H and ^{18}O) and unstable (^3H) isotope levels, as well as physical and chemical parameters (EC, Cl^-, NO_3^- and SO_4^{2-}), accounts for 64.08% of the variance, shows a certain degree of clustering. The points in red represent rainwater, green represents spring water, and blue represents borehole water.

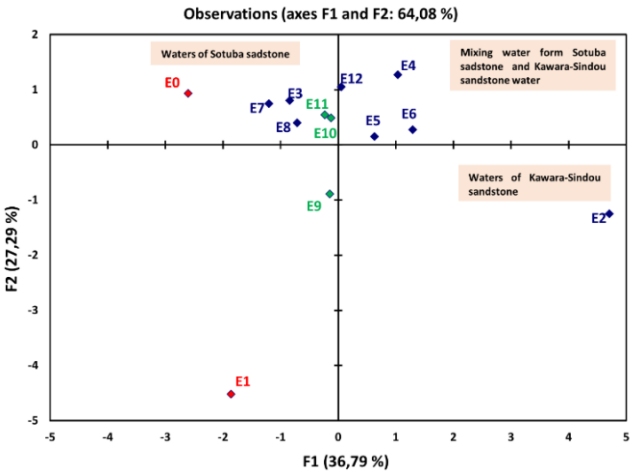

Figure 7. *Distribution of different types of water by observing the variables.*

There is a first grouping that includes waters E3, E7, and E8 (groundwater), and E10 and E11 (spring) on the one hand and a second grouping that includes E4, E5, E6, and E12 (groundwater) on the other. The first grouping consists of water from the Sotouba sandstone formations. Their proximity to rainwater indicates direct infiltration. They contrast with the second group, whose water comes from both the Sotouba sandstone and Kawara-Sindou sandstone formations (Figure 7).

The water from borehole E2 is completely different from the others. This water, originating from the Kawara-Sindou sandstone, is old and does not mix with current rainwater.

4.2. Environmental Tritium

The main origins of tritium present in the environment are: natural production mainly of atmospheric origin and artificial production due to thermonuclear tests in the atmosphere, from the 1960s [32]. An activity of less than 1 TU in West Africa corresponds to recharge before 1952.

The tritium content of groundwater, springs are of the same order of magnitude. Specifically, tritium contents of groundwater and sources vary between 1.8 TU and 3.66 TU with an average of 2.10 TU. This average indicates that the aquifers in the sector studied are at a very low renewal rate. Thus, compared to the average content of current rainwater in the area (5.22 TU), we note that only sample E9 (spring) in the aquifer Sotouba sandstone has a tritium content greater than 3 TU. This could be explained by the fact that this aquifer has a higher recharge rate compared to others (wells and springs), or that its waters may have been influenced by runoff, particularly since the sampling for analysis was conducted at the aquifer outlet during the rainy season. This observation could account for a direct and rapid recharge of rainwater that is very little influenced by evaporation phenomena. Based on the average tritium contents of current precipitation, we distinguish three families of water in the locality:

1) Contents greater than 3 TU: these contents correspond to those of recent water which are close to the contents of current rainwater.
2) Contents between 1.5 and 2.5 TU: These are mixtures of water between old water and recent water. This mixing of water would probably result from vertical exchanges which bring water from the underlying compartment along the geological accident [5, 32]. These upwelling phenomena are common in West Africa [40].
3) Contents less than 1 TU: These contents show old waters. We can estimate that the majority of water infiltrated before 1952 (start of thermonuclear tests).

Unlike the borehole, where the tritium values are concentrated around the mean, the spring's tritium values are concentrated above the mean (Figure 8).

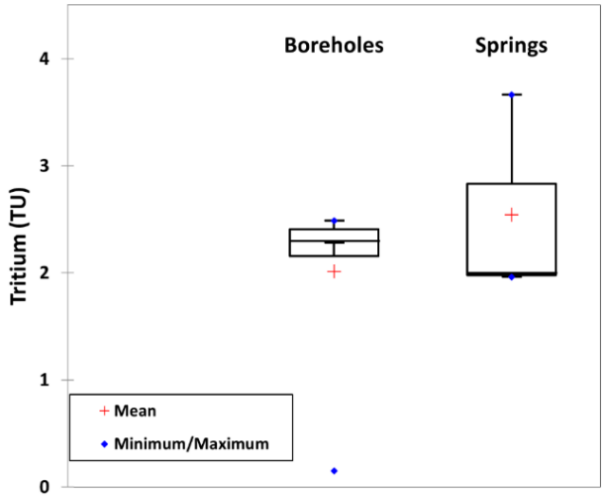

Figure 8. *Box plots show the variation in ^{3}H among samples from the springs and boreholes.*

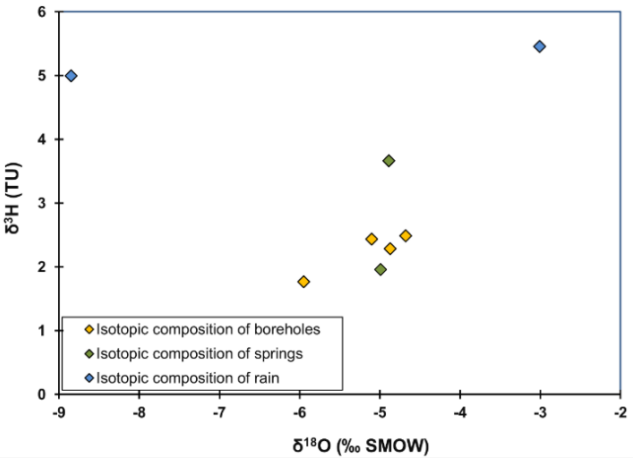

Figure 9. *Conventional diagram of $\delta^{3}H$ versus $\delta^{18}O$.*

Rainwater is highly enriched in ^{3}H, with values of 5 TU (July-August) and 5.5 TU (September-October). The depletion of ^{18}O isotopes in water during periods of heavy rainfall is marked. Some borehole and spring water seems to come from the same aquifer (Figure 9).

5. Discussion

The amount and intensity of rainfall are irregular during the rainy season (May to October). The heaviest rainfall in the study area typically occurs in July and August. The period from October to May represents the main dry season, with some precipitation due to convection or winter cyclonic disturbances.

The d-excess value in precipitation is lower than 10‰. This indicates either non-equilibrium conditions [30] or variations that probably depend mainly on vapour rather than the amount of precipitation due to the seasonal instability of evaporation, continental recycling and the relative humidity at the moisture

source [3, 41].

In the area, rainfall is more abundant in July and August, as shown by the value of d-excess (7.58), which is lower than that of September and October (8.4). This observation means that the value of excess deuterium depends on the amount of rainfall. Excess deuterium decreases with the abundance of rainfall. In other words, the higher the d-excess values, the greater the proportion of water evaporated in the precipitation [42]. Similar results have been reported in Burkina Faso, Cameroon, Bangladesh and Thailand [3, 5, 43, 44].

Groundwater d-excess values are high, with an average of 11.28‰, and all samples have values above the local precipitation average of 7.99‰. This result suggests direct infiltration by precipitation of oceanic and slightly continental origin, facilitated by a favourable geological context.

The stable isotopic composition appears to be influenced by the quantity effect and specific local meteorological conditions in tropical areas [3, 43, 45]. There is a depletion of ^{18}O and ^{2}H in rainwater from July-August, as opposed to September-October. This can be explained by the greater abundance of rainfall in July-August compared with September-October.

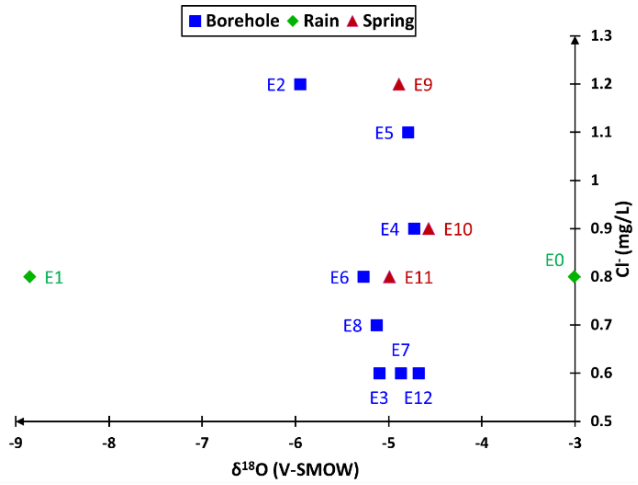

(a)

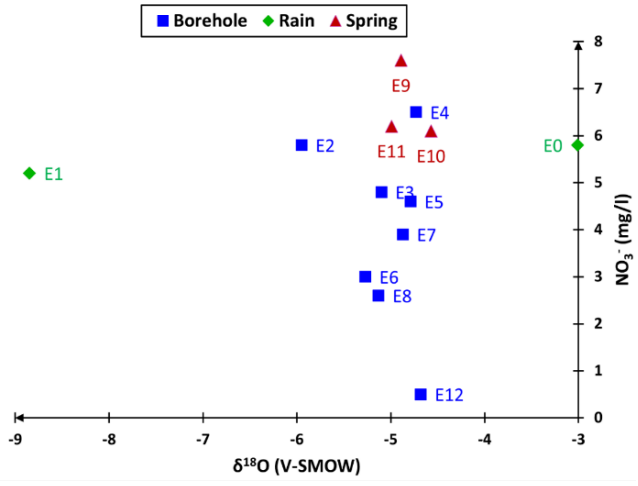

(b)

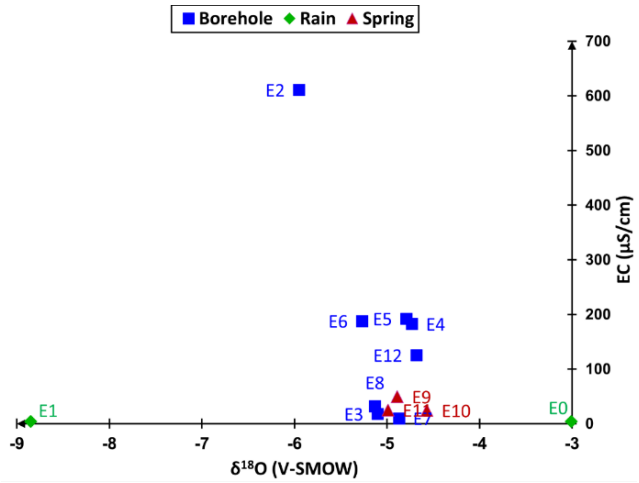

(c)

Figure 10. *The relationship between $\delta^{18}O$ and concentrations of a) chloride, b) nitrate and c) EC in groundwaters.*

The isotopic study reveals two distinct recharge periods: a cold, wet period characterized by a depletion of ^{18}O and the current period. Sample E2, which is the oldest with a tritium content of 1.8 TU, was recharged during this cold period. The other waters are the result of mixing with waters from the current period. This hypothesis is supported by the relationships between the levels of EC, Cl^- $NO_3^-$and $\delta^{18}O$ (V-SMOW). Specifically, communication between the E9 and E10 springs was not highlighted by the ^{18}O Vs Cl^- diagram, certainly because of the low quantities of Cl^- in the water tables. The springs are likely hydraulically conductive with the water from boreholes E3, E7 and E8, which tap the Sotouba sandstone geological formations. Boreholes E4, E5, and E6 do not communicate with the springs and therefore tap the Kawara Sindou sandstone aquifers. E12, the ONEA borehole, appears to tap both the Sotouba sandstone and Kawara Sindou sandstone aquifers (Figure 10).

The spring water originates from aquifers within the Sotouba sandstone geological formation, which has been exposed due to erosion.

6. Conclusion

This study was carried out to understand the functioning of the Pala aquifer system and the interaction between springs and groundwater. The stable isotopic composition (^{2}H and ^{18}O) of rainwater shows that it is practically unaffected by evaporation as it falls. Nevertheless, we have observed that the water becomes softer during heavy rainfall. The stable isotopic signature of the water from certain boreholes is therefore close to that of the actual rainwater in the study area, indicating direct and rapid infiltration of rainwater with very little influence from evaporation. The isotopic study indicates two distinct recharge periods: a cold, wet period with a depletion in ^{18}O, and the current period. Analysis of the radioactive isotopes of ^{3}H shows that the water in the boreholes

is not fossilized but is the result of mixing with present-day water. The springs observed in the study area originate from the Sotouba sandstone aquifers. They were created by erosion, which exposed the piezometric level of the water in the Kou basin, leading to these resurgences. Some boreholes tap aquifers from the two main geological formations, making it difficult to distinguish water from these two aquifers through analysis.

Abbreviations

ANAM	Agence Nationale de la Météorologie
DGRE	Direction Générale des Ressources en Eau
GMWL	Global Meteoric Water Line
IAEA	International Atomic Energy Agency
LMWL	Local Meteoric Water Line
LRAE	Laboratoire de Radio-Analyses et Environnement
ONEA	Office National de l'Eau et de l'Assainissement
SD	Standard Deviation
STBA	South-Eastern Taoudéni Basin Aquifer

Acknowledgments

The authors thank the Laboratoire de Radio-Analyses et Environnement of the Ecole Nationale d'Ingénieurs de Sfax (Tunisia) for performing the analysis and the anonymous reviewers for helpful comments improving this paper.

Author Contributions

César Millogo: Conceptualization, Data curation, Formal Analysis, Investigation, Methodology, Resources, Software, Visualization, Writing – original draft, Writing – review & editing

Issan Ki: Data curation, Software, Writing – review & editing

Issoufou Ouedraogo: Data curation, Software, Visualization, Writing – review & editing

Samuel Nakolendoussé: Project administration, Supervision, Validation

Data Availability Statement

The data is available from the corresponding author upon reasonable request.

Funding

This work is not supported by any external funding.

Conflicts of Interest

The authors declare no conflicts of interest.

References

[1] I. D. Clark et P. Fritz, *Environmental isotopes in hydrogeology*. Boca Raton, FL: CRC Press/Lewis Publishers, 1997.

[2] D. Dakouré, « Étude hydrogéologique et géochimique de la bordure Sud-Est du bassin sédimentaire de Taoudeni (Burkina Faso - Mali) - Essai de modélisation », Université Paris VI - Pierre et Marie Curie, Paris, 2003.

[3] H. C. Emvoutou *et al.*, « Hydrochemical and isotopic studies providing a new functional model for the coastal aquifers in Douala Coastal Sedimentary Basin (DCSB)/Cameroon », *Science of The Total Environment*, vol. 912, p. 169412, déc. 2023. https://doi.org/10.1016/j.scitotenv.2023.169412

[4] J. R. Gat, « Oxygen and hydrogen isotopes in the hydrologic cycle », 1996.

[5] I. KI, « Evaluation de la recharge des nappes souterraines du bassin de Tamassari (Bassin de Taoudéni) par l'utilisation des techniques spatiales (Géomatique), hydrogéochimiques et isotopiques », Ecole Nationale d'Ingénieurs de Tunis de l'Université Tunis El Manar et l'Université Joseph KI-ZERBO du Burkina Faso, Tunis et Ouagadougou, 2023.

[6] M. Kralik, « How to Estimate Mean Residence Times of Groundwater », *Procedia Earth and Planetary Science*, vol. 13, p. 301-306, 2015. https://doi.org/10.1016/j.proeps.2015.07.070

[7] P. Négrel et E. Petelet-Giraud, « Isotopes in groundwater as indicators of climate changes », *TrAC Trends in Analytical Chemistry*, vol. 30, n° 8, p. 1279-1290, Sept. 2011. https://doi.org/10.1016/j.trac.2011.06.001

[8] L. Araguas-Araguas, K. Froehlich, et K. Rozanski, « Deuterium and oxygen-18 isotope composition of precipitation and atmospheric moisture », *Hydrol. Process.*, vol. 14, n° 8, p. 1341-1355, juin 2000, https://doi.org/10.1002/1099-1085(20000615)14:8<1341::AID-HYP983>3.0.CO;2-Z

[9] S. Mahlangu, S. Lorentz, R. Diamond, et M. Dippenaar, « Surface water-groundwater interaction using tritium and stable water isotopes: A case study of Middelburg, South Africa », *Journal of African Earth Sciences*, vol. 171, p. 103886, nov. 2020. https://doi.org/10.1016/j.jafrearsci.2020.103886

[10] M. Masiol *et al.*, « Spatial distribution and interannual trends of δ18O, δ2H, and deuterium excess in precipitation across North-Eastern Italy », *Journal of Hydrology*, vol. 598, p. 125749, juill. 2021. https://doi.org/10.1016/j.jhydrol.2020.125749

[11] H. Wanke, M. Gaj, M. Beyer, P. Koeniger, et J. T. Hamutoko, « Stable isotope signatures of meteoric water in the Cuvelai-Etosha Basin, Namibia: Seasonal characteristics, trends and relations to southern African patterns », *Isotopes in Environmental and Health Studies*, vol. 54, n° 6, p. 588-607, nov. 2018. https://doi.org/10.1080/10256016.2018.1505724

[12] N. M. Dieng, P. Orban, J. Otten, C. Stumpp, S. Faye, et A. Dassargues, « Temporal changes in groundwater quality of the Saloum coastal aquifer », *Journal of Hydrology: Regional Studies*, vol. 9, p. 163-182, févr. 2017, https://doi.org/10.1016/j.ejrh.2016.12.082

[13] J. Ch. Fontes, «Environmental isotopes in groundwater hydrology», in *The Terrestrial Environment, A*, Elsevier, 1980, p. 75-140. https://doi.org/10.1016/B978-0-444-41780-0.50009-2

[14] S. Y. Ganyaglo *et al.*, «Groundwater residence time in basement aquifers of the Ochi-Narkwa Basin in the Central Region of Ghana», *Journal of African Earth Sciences*, vol. 134, p. 590-599, oct. 2017. https://doi.org/10.1016/j.jafrearsci.2017.07.028

[15] D. H. Madioune *et al.*, «Application of isotopic tracers as a tool for understanding hydrodynamic behavior of the highly exploited Diass aquifer system (Senegal)», *Journal of Hydrology*, vol. 511, p. 443-459, avr. 2014, https://doi.org/10.1016/j.jhydrol.2014.01.037

[16] M. Balasubramanian *et al.*, «Isotopic signatures, hydrochemical and multivariate statistical analysis of seawater intrusion in the coastal aquifers of Chennai and Tiruvallur District, Tamil Nadu, India», *Marine Pollution Bulletin*, vol. 174, p. 113232, 2022, https://doi.org/10.1016/j.marpolbul.2021.113232

[17] O. Dhaoui, I. M. H. R. Antunes, C. Boente, B. Agoubi, et A. Kharroubi, «Hydrogeochemical processes on inland aquifer systems: A combined multivariate statistical technique and isotopic approach», *Groundwater for Sustainable Development*, vol. 20, p. 100887, 2023. https://doi.org/10.1016/j.gsd.2022.100887

[18] K. A. R. Kpegli, A. Alassane, S. E. A. T. M. Van Der Zee, M. Boukari, et D. Mama, «Development of a conceptual groundwater flow model using a combined hydrogeological, hydrochemical and isotopic approach: A case study from southern Benin», *Journal of Hydrology: Regional Studies*, vol. 18, p. 50-67, août 2018. https://doi.org/10.1016/j.ejrh.2018.06.002

[19] A. Vengosh, J. Gill, M. Lee Davisson, et G. Bryant Hudson, «A multi‐isotope (B, Sr, O, H, and C) and age dating (^{3}H–^{3}He and ^{14}C) study of groundwater from Salinas Valley, California: Hydrochemistry, dynamics, and contamination processes», *Water Resources Research*, vol. 38, n° 1, janv. 2002. https://doi.org/10.1029/2001WR000517

[20] J. Derouane, «Modélisation hydrogéologique du bassin sédimentaire», SAWES-SOFRECO, 2008.

[21] D. Giovenazzo, A. Ouédraogo, K. A. A. HIEN, P. I. Ouédraogo, R. DAHL, et Y. SOUNTRA, «Carte de synthèse géologique, structurale et des substances minérales du Burkina Faso à 1/1 000 000», 2018.

[22] P. Gombert, «Synthèse sur la géologie et l'hydrogéologie de la zone sédimentaire RESO», RESO, 1998.

[23] C. Ouédraogo, «Synthèse géologique de la région ouest du Burkina Faso», 2006.

[24] SOGREAH Ingénierie, «Etude des ressources en eau souterraines de la région de Bobo Dioulasso», Sogreah, 1994.

[25] F. Huneau *et al.*, «Flow pattern and residence time of groundwater within the south-eastern Taoudeni sedimentary basin (Burkina Faso, Mali)», *Journal of Hydrology*, vol. 409, n° 1-2, p. 423-439, oct. 2011. https://doi.org/10.1016/j.jhydrol.2011.08.043

[26] G. Hottin et O. F. Ouédraogo, *Carte géologique à 1/1000000 de la République de Haute-Volta: Notice explicative*. Direction de la géologie et des mines, 1975. [En ligne]. Disponible sur: https://books.google.bf/books?id=jzy00AEACAAJ

[27] M. Talbaoui, «Etude des périmètres de protection des sources de Nasso et des forages de l'ONEA», SOFRECO-SAWES, Ouagadougou, 2009.

[28] T. B. Coplen, «Normalization of oxygen and hydrogen isotope data», *Chemical Geology: Isotope Geoscience section*, vol. 72, n° 4, p. 293-297, juin 1988. https://doi.org/10.1016/0168-9622(88)90042-5

[29] H. Craig, «Isotopic Variations in Meteoric Waters», *Science*, vol. 133, n° 3465, p. 1702-1703, mai 1961. https://doi.org/10.1126/science.133.3465.1702

[30] W. Dansgaard, «Stable isotopes in precipitation», *Tellus*, vol. 16, n° 4, p. 436-468, nov. 1964. https://doi.org/10.1111/j.2153-3490.1964.tb00181.x

[31] Y. Koussoube, «Hydrogéologie des séries sédimentaires de la dépression piézométrique du Gondo (bassin du Sourou): Burkina Faso / Mali», Université Paris VI - Pierre et Marie Curie, 264p, 2010.

[32] M. J. D. Taupin *et al.*, «Gestion intégrée et durable des systèmes aquifères et des bassins partagés de la région du Sahel», RAF/7/011, 2017.

[33] A. A. Barry, «Étude biogéochimique et isotopique dans les eaux souterraines au voisinage des décharges d'ordures en milieu fracturé et urbain: cas de la commune de Ouagadougou (Burkina Faso)», Université d'Avignon et Université Joseph KI-ZERBO, Ouagadougou, 258p, 2023.

[34] D. Adomako, A. Gibrilla, P. Maloszewski, S. Y. Ganyaglo, et S. P. Rai, «Tracing stable isotopes (δ2H and δ18O) from meteoric water to groundwater in the Densu River basin of Ghana», *Environ Monit Assess*, vol. 187, n° 5, p. 264, mai 2015. https://doi.org/10.1007/s10661-015-4498-2

[35] S. Valdivielso, J. Murray, E. Custodio, A. Hassanzadeh, D. E. Martínez, et E. Vázquez-Suñé, «Seasonal and isotopic precipitation patterns in the semi-arid and high mountain areas», *Science of The Total Environment*, vol. 925, p. 171750, 2024. https://doi.org/10.1016/j.scitotenv.2024.171750

[36] M. J. Wirmvem *et al.*, «Shallow groundwater recharge mechanism and apparent age in the Ndop plain, northwest Cameroon», *Appl Water Sci*, vol. 7, n° 1, p. 489-502, mars 2017. https://doi.org/10.1007/s13201-015-0268-0

[37] Z. Xia, J. Surma, et M. J. Winnick, «The response and sensitivity of deuterium and 17O excess parameters in precipitation to hydroclimate processes», *Earth-Science Reviews*, vol. 242, p. 104432, 2023. https://doi.org/10.1016/j.earscirev.2023.104432

[38] L. Gourcy, A. Brenot, et E. Petelet-Giraud, «Isotopic and geochemical tools for characterizing surface water-groundwater relationships in la Bassée floodplain area (Seine River Basin, France)», 2011.

[39] L. Gourcy, J.-F. Aranyossy, J.-C. Olivry, et G. M. Zuppi, « Évolution spatio-temporelle des teneurs isotopiques (δ2H–δ18O) des eaux de la cuvette lacustre du fleuve Niger (Mali) », 2000.

[40] A. M. S. Babaye, « Evaluation des ressources en eau souterraine dans le bassin de Dargol (Liptako – Niger) », Université de Liège et Université Abdou Moumouni, Liège, 2012.

[41] P. D. Sreedevi, P. D. Sreekanth, et D. V. Reddy, « Deuterium Excess of Groundwater as a Proxy for Recharge in an Evaporative Environment of a Granitic Aquifer, South India », *J Geol Soc India*, vol. 97, n° 6, p. 649-655, juin 2021. https://doi.org/10.1007/s12594-021-1740-0

[42] A. L. Putman, R. P. Fiorella, G. J. Bowen, et Z. Cai, « A Global Perspective on Local Meteoric Water Lines: Meta-analytic Insight Into Fundamental Controls and Practical Constraints », *Water Resources Research*, vol. 55, n° 8, p. 6896-6910, août 2019. https://doi.org/10.1029/2019WR025181

[43] M. R. Islam *et al.*, « Controls on spatiotemporal variations of stable isotopes in precipitation across Bangladesh », *Atmospheric Research*, vol. 247, p. 105224, janv. 2021. https://doi.org/10.1016/j.atmosres.2020.105224

[44] C. Sun, S. Zhou, et Z. Jing, « Variability of precipitation-stable isotopes and moisture sources of two typical landforms in the eastern Loess Plateau, China », *Journal of Hydrology: Regional Studies*, vol. 46, p. 101349, 2023. https://doi.org/10.1016/j.ejrh.2023.101349

[45] F. Ma, J. Chen, J. Chen, et T. Wang, « Environmental drivers of precipitation stable isotopes and moisture sources in the Mongolian Plateau », *Journal of Hydrology*, vol. 621, p. 129615, 2023. https://doi.org/10.1016/j.jhydrol.2023.129615